

A Clinical Prototype for Microwave Breast Imaging Using Time-Domain Measurements

Emily Porter, Evgeny Kirshin, Adam Santorelli, Milica Popović

Department of Electrical Engineering, McGill University, Montreal, Canada, {emily.porter, evgeny.kirshin, adam.santorelli}@mail.mcgill.ca, milica.popovich@mcgill.ca

Abstract—This work presents a clinical prototype for microwave breast imaging via multistatic radar using time-domain measurements. The imaging system involves a 16-element broadband antenna array that is integrated into a table for ease of interfacing with patients. We briefly describe the imaging system and discuss its incorporation into a tool appropriate for patient use, focusing on both medical and practical aspects. Further, we demonstrate the functionality of the complete system by reconstructing images of malignant tissues within realistically shaped and sized breast models.

Index Terms—*Biomedical imaging, cancer detection, microwave imaging, multistatic radar.*

I. INTRODUCTION

Microwave methods for breast cancer detection and monitoring have been the focus of significant research attention over the past decade. Microwave techniques offer a promising complementary modality for breast imaging, as they have the potential for low-cost and pain-free scans without the harmful ionizing radiation that is used in the standard imaging method of x-ray mammography. A variety of breast imaging systems using microwaves have been reported to date; several clinically ready systems operating with frequency-domain measurements have been developed [1] – [4], and while a few systems using time-domain recordings have been investigated [5] – [9], to the best of our knowledge no such systems have reached the clinical prototype stage. Time-domain measurement systems are thought to offer potential advantages over systems that record in the frequency domain, including decreased complexity in signal processing, faster scan speeds, and improved cost-effectiveness [5]. However, measurement systems that operate in the frequency-domain offer higher signal to noise ratio [5], indicating that the trade-off in the aforementioned factors should be optimized.

Our multistatic radar system, which utilizes time-domain measurements, was presented in a basic form in [6]. This work focuses on the clinical implementation of our improved breast imaging system. The development and application of the clinical system, described here in detail, take into consideration key practical factors including sanitization, patient comfort, mobility (ease of transport), and cost-effectiveness. In the following section, the imaging system itself is described. Next, the integration of the system into the patient interface is

examined. Finally, we demonstrate the imaging functionality by showing a sample reconstructed breast image.

II. BACKGROUND

A. Time-Domain Measurement System

The time-domain measurement system is composed of a pulse generator, pulse-shaping circuitry, a 16-element broadband antenna array, and an oscilloscope. A description of the basic system components (without a full antenna array) is provided in [6]. The system is designed to operate over the 2 - 4 GHz range. The breast under test is held in a hemispherical bowl-shaped radome, the exterior of which houses the antenna array. In between the breast and the radome wall is a thin layer of ultrasound gel, used to avoid air gaps and attenuate undesirable multiple reflections between the skin and the radome.

Our system operates based on a differential comparison method between past and current scans. The idea is that scans can be completed at regular intervals and the presence of developing malignancies would then be determined by comparing current data to previously obtained data. This method has been shown to be a viable approach for microwave breast imaging [8]. In particular, in the simplified test presented here, we take complete breast scans before and after the breast phantom has ‘developed’ a malignancy. The two scans contain 240 signals each (16 transmitting antennas x 15 remaining antennas as receivers). The data is time-aligned and normalized, and then corresponding signals from the two scans are compared to remove the direct pulse (the component of the signal that passes directly from transmitter to receiver without passing through the tumour or reflecting off it). This processing results in a set of ‘tumour response signals’, i.e., the contributions to the original signals that were caused by the presence of the tumour. It is these tumour response signals that are used to generate images.

B. Breast Phantoms

We use breast models that are shaped and sized as a typical average breast. They contain tissue phantoms with dielectric properties matched, over the microwave frequency range of interest, to those of actual breast tissues. These realistically shaped phantoms have dimensions of 17.5 cm x 16.5 cm x 8 cm, at the widest section. They are composed of a textured

This work was supported by the Natural Sciences and Engineering Research Council of Canada (NSERC), le Fonds québécois de la recherche sur la nature et les technologies (FQRNT) and Partenariat de Recherche Orientée en Microélectronique, Photonique et Télécommunications (PROMPT).

skin layer approximately 2 mm thick, filled with fat-mimicking material and tumour(s). The tumours can be of any chosen shape and size, and are easily placed at any desired locations. Descriptions of the tissue phantoms fabrication process, and measurements of their dielectric properties are reported in [10]. Photographs of the complete, realistically shaped phantoms can be found in [11].

III. CLINICAL SETUP

We integrate the measurement system into a soft, padded table on which the patient can lie for the duration of the breast scan. The system is designed for a patient lying in the prone position. A hole is cut into the table in which the radome is placed; the table structure holds the radome securely in position. Underneath the radome, all measurement equipment sits on a movable shelf rack. On the top shelf, closest to the antennas, is the switching matrix. The pulse generator, pulse-shaping circuitry, oscilloscope and clock are also located on the shelf rack. The computer can be controlled remotely to avoid having technical personnel in the vicinity of the patient. A photograph of the measurement system and patient interface is shown in Fig. 1.

The design of the patient table included several factors, limited not only to those of electrical concern, but also to practical matters including patient well-being and physical/mechanical challenges. Key considerations, which were factored into the patient interface design and layout, are listed as follows: portability, ease of use, patient comfort, sanitization between patients, cost-effectiveness, and integrity and repeatability in the measurement system. In particular, the table folds up and can be put away quickly, requiring only a small area for storage. It can be reassembled in less than 10 minutes. Further, the measurement system is placed on a wheeled rack that allows for easy relocation, and the antennas can be permanently fixed in the radome so that no measurement discrepancies occur due to antenna movements (this was shown in [3] to be a contributing factor to differences between calibration signals and collected data). The table setup does not include any metal components or any other materials that would interfere with the microwave signals used in measurements. The measurement system uses ultrasound gel as a breast immersion medium, a product that is already approved for medical use and is readily available with little expense. Additionally, the table incorporates an easy to sterilize vinyl padding cover with removable, washable blankets and pillow covers. Finally, the patient interface was designed with comfort in mind – the table is well padded, and a complete breast scan currently takes less than 18 minutes.

IV. IMAGING RESULTS

A sample reconstructed image of a realistically shaped breast phantom is shown in Fig. 2. In this example, an approximately spherical tumour with radius of 1 cm was placed in the left hemisphere of the breast phantom. In the image, red indicates strongly scattered electromagnetic energy, whereas blue represents less scattering; we also note that the energy is plotted on a linear scale. From Fig. 2, it is clear that the tumour appears as the largest scatterer of electromagnetic energy within the phantom.



Fig. 1. Photograph of the breast imaging measurement system and its patient interface.

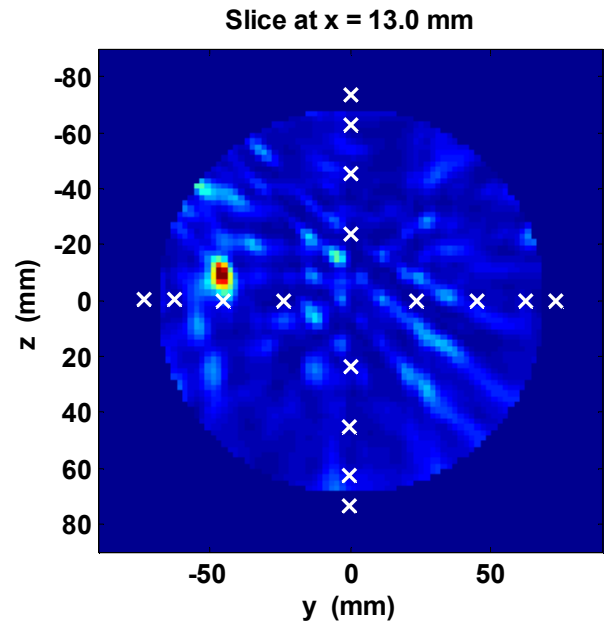


Fig. 2. Coronal slice from a reconstructed image of a breast phantom. The “x” markers represent the positions of the antennas. Slice depth ($x = 13$ mm) is measured from the chest wall towards the nipple.

In order to further examine the reconstructed image, we introduce two metrics that show the quality of the tumour detection. These parameters are the tumour localization error and the signal-to-clutter ratio. We define the tumour localization error as the distance between the physical centre of the tumour and the location where the maximum scatterer appears in the image. In all results shown here, the tumour appears in the image at the correct depth range, so the localization error is the remaining offset composite of only the y and z dimensions. We note that the calculated localization error is not overly accurate due to the manual placement of the tumour within the phantom such that its position cannot be

controlled down to a millimetre-level. The signal-to-clutter ratio (SCR), measured in dB, is the ratio between the scattered intensity at the tumour location and the next highest intensity. These metrics allow us to determine the ease of the system's ability to detect the tumour – a high SCR indicates that the presence of a tumour is easily detected, and a low localization error suggests that the position of the tumour is accurately depicted in the reconstructed images.

In the example presented in Fig. 2, the tumour is localized to within 9.2 mm and the signal-to-clutter ratio is 6.8 dB. These values suggest that the time-domain imaging system is working as designed, and thus the tumour can be successfully seen in the images. The localization error can potentially be improved by both increasing the number of antennas around the radome and distributing them evenly, as well as by better estimating tissue properties in the imaging algorithm. The signal-to-clutter ratio can be increased by better clutter suppression and removal of background noise, among other methods. We are currently working on solutions that will enhance both of these parameters in order to allow us to successfully image more complex, heterogeneous breasts.

V. CONCLUSIONS

We have demonstrated a clinically ready time-domain microwave breast imaging system and tested it with a realistically shaped breast phantom. The proposed system is designed to be portable, comfortable and sanitary for the patient, and to have all measurement components fixed securely to ensure consistency between measurements. We provide a sample image reconstructed from a homogeneous, realistically shaped breast phantom with skin and show that the tumour is easily seen. Future work includes increasing the number of antennas to improve the tumour localization, and methods to better the signal-to-clutter ratio. Tests on complex heterogeneous phantoms and volunteers are also a next step towards examining the feasibility of this type of time-domain microwave breast imaging system.

ACKNOWLEDGMENT

The authors thank Jules Gauthier at Polytechnique Montreal for fabricating the antennas. We are also grateful to the

McGill Photonic Systems Group for allowing us access to lab space and the equipment necessary for making the breast phantoms.

REFERENCES

- [1] M. Klemm, et al., "Development and testing of a 60-element UWB conformal array for breast cancer imaging," *Antennas and Propagation (EUCAP), Proceedings of the 5th European Conference on*, pp. 3077 – 3079, Rome, Italy, Apr. 11-15, 2011.
- [2] P. M. Meaney, M. W. Fanning, D. Li, S. Poplack, and K. D. Paulsen, "A clinical prototype for active microwave imaging of the breast" *IEEE Trans Microw. Theory Techn.*, vol. 48, no. 11, Nov. 2000.
- [3] J. Bourqui, J. M. Sill, and E. C. Fear, "A prototype system for measuring microwave frequency reflections from the breast," *Int. J. Biomedical Imaging*, vol. 2012, 2012.
- [4] X. Li, E. J. Bond, B. D. V. Veen, and S. C. Hagness, "An overview of ultra-wideband microwave imaging via space-time beamforming for early-stage breast-cancer detection," *IEEE Antennas Propag. Mag.*, vol. 47, no. 1, pp. 19–34, Feb. 2005.
- [5] X. Zeng, A. Phager, P. Linner, M. Persson, and H. Zirath, "Experimental investigation of the accuracy of an ultrawideband time-domain microwave-tomographic system," *IEEE Trans. Instrum. Meas.*, vol. 60, no. 12, Dec. 2011.
- [6] E. Porter, A. Santorelli, M. Coates, and M. Popović, "Time-domain microwave breast cancer detection: extensive system testing with phantoms," *Technol Cancer Res Treat.*, 2012 [Epub ahead of print].
- [7] J. C. Y. Lai, C. B. Soh, E. Gunawan, and K. S. Low, "UWB microwave imaging for breast cancer detection – experiments with heterogeneous breast phantoms," *Prog. Electromagn. Res. M*, vol. 16, pp. 19-29, 2011.
- [8] D. Byrne, M. O'Halloran, M. Glavin, and E. Jones, "Breast cancer detection based on differential ultrawideband microwave radar," *Prog. Electromagn. Res.*, vol. 20, pp. 231 – 242, 2011.
- [9] W. Liu, H. M. Jafari, S. Hranilovic, and M. J. Deen, "Time domain analysis of UWB breast cancer detection," *Communications, 2006 23rd Biennial Symposium on*, pp. 336 – 339, Kingston, Canada, May 30 – June 1, 2006.
- [10] A. Santorelli, "Breast screening with custom-shaped pulsed microwaves," *M. Eng. Thesis, Dept. Elec. and Comp. Eng., McGill Univ.*, Montréal, Canada, 2012.
- [11] E. Porter, A. Santorelli, S. Winkler, M. Coates, and M. Popović, "Time-domain microwave cancer screening: optimized pulse shaping applied to realistically shaped breast phantoms," *Microwave Symposium Digest (MTT), 2012 IEEE MTT-S International*, Montréal, Canada, pp. 1 – 3, June 17 – 22, 2012.